ehp ENVIRONMENTAL HEALTH PERSPECTIVES
http://www.ehponline.org

Interlaboratory Evaluation of *in Vitro* Cytotoxicity and InflammatoryResponses to Engineered Nanomaterials: The NIEHS NanoGo Consortium

Tian Xia, Raymond F. Hamilton Jr, James C. Bonner, Edward D. Crandall, Alison Elder, Farnoosh Fazlollahi, Teri A. Girtsman, Kwang Kim, Somenath Mitra, Susana A. Ntim, Galya Orr, Mani Tagmount, Alexia J. Taylor, Donatello Telesca, Ana Tolic, Christopher D. Vulpe, Andrea J. Walker, Xiang Wang, Frank A. Witzmann, Nianqiang Wu, Yumei Xie, Jeffery I. Zink, Andre Nel and Andrij Holian

http://dx.doi.org/10.1289/ehp.1306561

Online 06 May 2013

NIH National Institute of Environmental Health Sciences

Interlaboratory Evaluation of *in Vitro* Cytotoxicity and Inflammatory Responses to Engineered Nanomaterials: The NIEHS NanoGo Consortium

Tian Xia[1], Raymond F. Hamilton Jr[2], James C. Bonner[3], Edward D. Crandall[4], Alison Elder[5], Farnoosh Fazlollahi[4], Teri A. Girtsman[2], Kwang Kim[4], Somenath Mitra[6], Susana A. Ntim[6], Galya Orr[7], Mani Tagmount[8], Alexia J. Taylor[3], Donatello Telesca[1], Ana Tolic[7], Christopher D. Vulpe[8], Andrea J. Walker[5], Xiang Wang[1], Frank A. Witzmann[9], Nianqiang Wu[10], Yumei Xie[7], Jeffery I. Zink[1], Andre Nel[1], and Andrij Holian[2]

[1]Department of Medicine, Division of NanoMedicine, Center for Environmental Implications of Nanotechnology, California Nanosystems Institute, University of California at Los Angeles, Los Angeles, California, USA

[2]Center for Environmental Health Sciences, Department Biomedical and Pharmaceutical Sciences, University of Montana, Missoula, Montana, USA

[3]Department of Environmental and Molecular Toxicology, North Carolina State University, Raleigh, North Carolina, USA

4Department of Medicine, University of Southern California, Los Angeles, California, USA

[5]Department of Environmental Medicine, University of Rochester, Rochester, New York, USA

[6]Department of Chemistry and Environmental Science, New Jersey Institute of Technology, Newark, New Jersey, USA

[7]Environmental Molecular Sciences Laboratory, Pacific Northwest National Laboratory, Richland Washington, USA

[8]Department of Nutritional Science and Toxicology, University of California, Berkeley, Berkeley, California, USA

[9]Department of Cellular & Integrative Physiology, Indiana University School of Medicine, Indianapolis, Indiana, USA

[10]Department of Mechanical and Aerospace Engineering, West Virginia University, Morgantown, West Virginia, USA

Correspondence: Andrij Holian, andrij.holian@mso.umt.edu, 280 Skaggs Building, Center for Environmental Health Sciences, 32 Campus Drive, The University of Montana, Missoula, MT 59812 (406) 243-4018

Keywords: cell viability, inflammation, *in vitro*, MWCNT, nanotoxicology, round robin testing, TiO_2, ZnO

Running Title: NanoGo Consortium *in vitro* Testing of Nanomaterials

Funding: The authors would like to acknowledge the support from the following American Recovery and Reinvestment Act (ARRA) grants: RC2 ES018742 (AH), RC2 ES018810 (FW), RC2 ES018786 (GO), RC2 ES018772 (JCB), RC2 ES018766 (AN), RC2 ES018812 (CV), RC2 ES018741 (AE), and RC2 ES018782 (EDC). Support was also provided by Centers of Biomedical Research Excellence (COBRE) grant P20 RR017670 (AH).

Acknowledgements: The authors appreciate the excellent technical assistance provided by Mary Buford (University of Montana), Heather Ringham and Meixian Fang (Indiana University) and Nancy Corson (University of Rochester). The authors thank Dr. Srikanth Nadadur, Program Director at the NIEHS Division of Extramural Program for initiation and direction of these consortium efforts. We also thank Dr. Thaddeus Schug at NIEHS for administrative organization and planning of consortium conferences.

Disclaimers: There were no competing financial interests.

Abbreviations:

BEGM Bronchial epithelial growth medium

BET Brunauer, Emmett and Teller

DLS Dynamic light scattering

ENM Engineered Nanomaterial

ICP-MS inductively coupled plasma mass spectrometry

IL-1β Interleukin-1β

LDH Lactate Dehydrogenase

MTS (3-(4,5-dimethylthiazol-2-yl)-5-(3-carboxymethoxyphenyl)-2-(4-sulfophenyl)-2H-tetrazolium)

MWCNT Multi-Walled Carbon Nanotube

O-MWCNT Original MWCNT

F-MWCNT Functionalized MWCNT

P-MWCNT Purified MWCNT

SEM Scanning electron microscopy

TEM Transmission electron microscopy

TiO_2 Titanium Dioxide

TiO_2-A Anatase TiO_2

TiO_2-P25 Rutile/Anatase TiO_2

TiO_2-NB TiO_2 Nanobelts

XRD x-ray defraction

Abstract

Background: Differences in interlaboratory research protocols contribute to the conflicting data in the literature regarding engineered nanomaterial (ENM) bioactivity. Therefore, grantees of a NIEHS-funded consortium program performed two phases of *in vitro* testing with selected ENM in an effort to identify and minimize sources of variability.

Methods: Consortium Program Participants (CPP) conducted ENM bioactivity evaluations on ZnO, three forms of TiO_2, and three forms of multiwalled carbon nanotubes (MWCNT). In addition, CPP performed bioassays using three mammalian cell lines (BEAS-2B, RLE-6TN, and THP-1) selected in order to cover two different species (rat and human), two different lung epithelial cells (alveolar type II and bronchial epithelial cells), and two different cell types (epithelial cells and macrophages). CPP also measured cytotoxicity in all cell types while measuring inflammasome activation (IL-1β release) only using THP-1 cells.

Results: The overall *in vitro* toxicity profiles of ENM were: ZnO was cytotoxic to all cell types at 50 μg/mL or higher, but did not induce IL-1β. TiO_2 was not cytotoxic except for the nanobelt form, which was cytotoxic and induced significant IL-1β production in THP-1 cells. MWCNT did not produce cytotoxicity, but stimulated lower levels of IL-1β production in THP-1 cells, with the original MWCNT producing the most IL-1β.

Conclusions: The results provided justification for the inclusion of mechanism-linked bioactivity assays along with traditional cytotoxicity assays for *in vitro* screening. In addition, the results suggest that conducting studies with multiple relevant cell types to avoid false negative outcomes is critical for accurate evaluation of ENM bioactivity.

Introduction

The worldwide development of innovative products increasingly includes incorporation of engineered nanomaterials (ENM). It is likely that ENM use will become ever more commonplace in the future and provide many benefits although harm from inadvertent human exposures may also increase. There are challenges in evaluation of ENM safety that need to be addressed, especially considering that the pace of ENM development is exceeding the industry's ability to sufficiently conduct animal safety testing (Maynard et al. 2006; Nel et al. 2006; Oberdorster et al. 2005). To address this issue, one of the goals in the field of nanotoxicology (or nanosafety) is development of *in vitro* assays that are highly predictive of *in vivo* outcomes in order to triage those ENM that should proceed to *in vivo* testing (Meng et al. 2009; Oberdorster et al. 2005). Unfortunately, the presence of conflicting interlaboratory data on the relative hazard of individual ENM is a concern for moving the reliability of *in vitro* testing forward. Therefore, the National Institute of Environmental Health Sciences (NIEHS) developed a consortium program of experts in the field of pulmonary toxicology to conduct coordinated *in vitro* and *in vivo* assays with selected well-characterized ENM. There are a number of potential causes of variability including: sources of ENM, ENM suspension protocols, selection of target cells, endpoints selected to evaluate ENM bioactivity, and details of cell culture and endpoint assays.

All CPP received characterized ENM for use in this study, including metal oxide nanospheres (TiO_2-P25, TiO_2 Anatase (TiO_2-A), and ZnO) and high aspect ratio materials (multiwalled carbon nanotubes (MWCNT) and TiO_2-nanobelts (TiO_2-NB)). Furthermore, the CPP tested three forms of MWCNT (original (O-MWCNT), purified (P-MWCNT) and functionalized (carboxylated) (F-MWCNT)). The CPP chose cell lines for the assays based on

respiratory tract exposure, thus, the cell types most likely to interact with ENM after deposition. As such, the cell lines include RLE-6TN (rat type II alveolar epithelial cell line), BEAS-2B (human lung bronchial epithelial cell line) and THP-1 (human monocyte/macrophage cell line) (Dostert et al. 2008; Driscoll et al. 1995; Xia et al. 2008b). CPP developed ENM suspension protocols (in cell culture media) that were sufficiently reproducible amongst laboratories (Ji et al. 2010; Porter et al. 2008; Sager et al. 2007). The cell assays included traditional cytotoxicity testing (Xia et al. 2008b), and evaluation of the Nod-like receptor protein 3 (NLRP3) inflammasome activation with THP-1 cells (Hamilton et al. 2009). The CPP chose the inflammasome assay based on evidence that a number of particles such as crystalline silica, asbestos, uric acid crystals, and cholesterol crystals activate the NLRP3 inflammasome causing the release of Interleukin-1β (IL-1β) and IL-18 that have been linked to lung pathology (Cassel et al. 2008; Dostert et al. 2008; Franchi et al. 2009; Tschopp and Schroder 2010). For example, a laboratory from the CPP recently showed that TiO_2-NB stimulate the NLRP3 inflammasome in primary murine macrophages (Hamilton et al. 2009). This manuscript describes the outcomes of the *in vitro* consortium, while a companion paper (Bonner et al. 2013) describes the *in vivo* studies conducted in rodents using the same well-characterized ENM.

This study identified and minimized critical aspects of current ENM testing protocols that will potentially decrease the variability in reported outcomes from the various labs engaged in the field. In addition, the study provides new information on the relative *in vitro* bioactivity of a large group of diverse ENM that can be used to inform future strategies for *in vitro* testing and predicting *in vivo* outcomes.

Materials and Methods

ENM and Reagents

The CPP obtained ZnO from Meliorum Inc. TiO_2-P25 is 81% anatase and 19% rutile, purchased from Evonik (Parsippany, NJ). Dr. Pratim Biswas provided the TiO_2-A (Washington University, St. Louis). The CPP prepared the TiO_2-NB as previously described (Hamilton et al. 2009) and purchased the O-MWCNT stock in powder form from Cheap Tubes, Inc. (Brattleboro, VT). The CPP obtained P-MWCNT by treatment of O-MWCNT with dilute acids, chelating agents, and mild conditions to minimize oxidized or damaged tubes. Further acid treatment of P-MWCNT introduced carboxyl groups on 5.27% of the carbon backbone (on a per weight basis) to create F-MWCNT (Chen and Mitra 2008; Wang et al. 2011).

The CPP purchased low-endotoxin bovine serum albumin from Gemini Bio-Products (West Sacramento, CA), and Dipalmitoylphosphatidylcholine, phorbol 12-myristate, 13-acetate (PMA), and lipopolysaccharide (LPS from Escherichia coli 0127:B8) from Sigma-Aldrich (St. Louis, MO). EMD Millipore (Billerica, MA) vended the 1,25-dihydroxy-vitamin D_3. The CPP purchased the Cytotoxicity assays CellTiter 96 (MTS assay) and CytoTox 96 (LDH assay) from Promega (Madison, WI).

Preparation of ENM in cell culture media

The CPP made up ENM stock solutions (5 mg/ml) from dry powder using endotoxin free sterile water and then freshly prepared all ENM suspensions in cell culture media using the stock solutions. Briefly, the CPP vortexed then sonicated ENM stock solutions (with the exception of TiO_2-NB, which were stirred to prevent mechanical shear) using a water bath sonicator or cup

horn sonicator (depending on lab availability) immediately before diluting into complete cell culture medium.

Cell Culture and Co-incubation with EMN

The CPP grew cells at 37°C in a 5% CO_2 atmosphere. In addition, the CPP obtained the RLE-6TN cells, a rat alveolar type II epithelial cell line, from American Type Culture Collection (ATCC, Manassas, VA) and cultured in Ham's F12 medium (ATCC) supplemented with L-glutamine, bovine pituitary extract (BPE), insulin, insulin growth factor (IGF)-1, transferrin and epithelial growth factor (EGF), supplemented with 10% fetal bovine serum (FBS). The CPP obtained THP-1 cells, a human acute monocytic leukemia cell line, from ATCC and cultured in HEPES-buffered RPMI 1640 supplemented with L-glutamine (Mediatech, Corning, NY), 0.05 mM beta-mercaptoethanol and 10% FBS. PAA Laboratories (Dartmouth, MA) vended the FBS for THP-1 cells. The CPP obtained BEAS-2B cells from ATCC, and cultured them in Bronchial epithelial growth medium (BEGM) obtained from Lonza Inc. (Walkersville, MD), and supplemented with BPE, insulin, hydrocortisone, human EGF, epinephrine, triiodothyronine, transferrin, gentamicin/amphotericin-B and retinoic acid. For the THP-1 differentiation performed in the first series of experiments (Phase I), the CPP pretreated cells with 1.62 μM (1 μg/ml) PMA for 18 h. However, the CPP identified excessive cell clumping and cell death during the Phase I studies. Therefore, the CPP alternatively pretreated THP-1 cells with Vitamin D_3 at 150 nM overnight and then 5 nM PMA in order to obtain the differentiated macrophage-like cells used during the second series of experiments (Phase II). For the IL-1β release, co-culturing THP-1 cells with 10 ng/mL LPS was necessary to initiate transcription of pro-IL-1β. The CPP initiated aggressive phagocytic activity by the addition of PMA just prior to particle exposure.

Before ENM exposure, the CPP cultured aliquots of 1.5×10^4 cells (for THP-1 cells, 10^5 cells were seeded into each well of a 96-well plate) in 0.2 mL of the cell culture media in 96-well plates (Costar, Corning, NY) at 37°C for 24 h. The CPP freshly prepared all of the ENM suspensions at final concentrations of 10, 25, 50, and 100 μg/mL in the cell culture media. Following exposure to the ENM for 24 h at 37°C, the CPP collected supernatants to measure LDH and IL-1β production then used the remaining cells to test cellular viability by MTS assay.

Physicochemical Characterization of ENM

The CPP identified the primary particle size and morphology of the ENM by using a transmission electron microscope (JEOL 100 CX TEM, Japan) and a scanning electron microscope (SEM, JSM-7600F, Japan). In addition, the CPP characterized the particle hydrodynamic size in H_2O and cell culture media using dynamic light scattering (DLS) (Ji et al. 2010). The CPP characterized particle crystallinity and structure using X-ray diffraction measurements and measured particle surface area by BET. The CPP performed Zeta-potential measurements of the ENM suspensions using a ZetaSizer Nano-ZS instrument (Malvern Instruments, Worcestershire WR, UK). Finally, the CPP determined the elemental composition of the particles as well as ZnO dissolution rate using inductively coupled plasma mass spectrometry (ICP-MS, Perkin-Elmer SCIEX Elan DRCII, USA).

Endotoxin analysis of ENM

CPP measured the endotoxin content of ENM stock suspensions, as well as dispersions in PBS and tissue culture media using the colorimetric Limulus amebocyte lysate assay (Lonza Inc., Walkersville, MD). The LPS content of all ENM suspensions was < 0.3 EU/mL.

Determination of cell viability

The CPP determined cellular viability using MTS (CellTiter 96, Promega, Madison WI) and LDH (CytoTox 96, Promega, Madison, WI) according to the manufacturer's protocols. In order to avoid the interference created by ENM while measuring formazan absorbance at 490 nm, the CPP introduced a centrifugation (2000 x g for 10 min) procedure in Phase II experiments to collect particles in the wells after incubation with the MTS reagents. CPP then followed this additional centrifugation step with a brief mixing and transfer of the supernatant to a new 96-well plate prior to measuring the formazan absorbance at 490 nm. The CPP eliminated interference of any residual LDH in FBS by heat-inactivation (70°C water bath for 5 min).

ELISA for IL-1β Quantification

The CPP determined IL-1β production in the THP-1 culture supernatant using a human IL-1β ELISA kit (R & D Systems Human IL-1β DuoSet™, CA, USA) following manufacturer's instructions.

Statistical Analysis

The CPP used the 2-way ANOVA followed by Turkey or Bonferroni correction for multiple comparisons of means for statistical analysis of responses across ENM and cell lines. In order to define inter-lab comparisons across two harmonization rounds, the CPP conducted a meta analysis of LDH, MTS and IL-1β assays across 8 different labs, for three cell lines (BEAS-2B, RLE-6TN and THP-1) exposed to several ENM (MWCNT, ZnO, TiO_2-P25, TiO_2-A, TiO_2-NB). The CPP combined information within assays and cell lines using a robust two-stage hierarchical model of toxicity. For all quantities of interest, the CPP obtained Monte Carlo inference by implementing a custom Gibbs sampler in the R computing environment (R Development Core

Team, 2009). In order to normalize data, the CPP subtracted background negative control values (MTS, LDH and IL-1β) and provided adjustments for positive control values in the case of LDH assays. The CPP has provided details about the statistical model used for analysis in the Supplemental Materials section.

Results

Physicochemical characterization of consortium ENM

CPP selected two types of nanomaterials for the studies in order to evaluate a sufficient number of material types. One type were metal oxides including TiO_2 (P25), TiO_2 (anatase), TiO_2 (nanobelts) and ZnO; while the other were three multiwall carbon nanotubes (MWCNT). A key element of this study was that all of the investigators used the same sets of ENM, which were extensively characterized a priori. Representative SEM images show the morphology of the different ENM: TiO_2-P25, TiO_2-A, and ZnO were spherical, TiO_2-NB were straight long fibers, O-MWCNT, P-MWCNT and F-MWCNT were long fibers (Figure 1). The CPP additionally characterized the ENM to determine size, surface area, crystal structure and purity (Tables 1 and 2). To determine the hydrodynamic size and charge of these materials, the CPP used both water and cell culture media respectively (Tables 1 and 2 *in water*; Supplemental Material, Tables S1 and S2 *in media*). Functionalization of MWCNT increased the negative surface charge in water, as would have been predicted. It should be noted that hydrodynamic diameters for non-spherical particles like nanotubes and nanowires are defined as the equivalent spherical diameters, *i.e.*, the diameter of a sphere with the same translational diffusion coefficient, and cannot be simply related to the exact particle sizes. Therefore, the hydrodynamic diameters measured here for TiO_2-NB and MWCNT only represent their "relative" sizes. DLS measurements provide a good

indication of the dispersion state of high aspect ratio ENM, like MWCNT (Wang et al. 2010) and CeO_2 nanorods and nanowires (Ji et al. 2012). For MWCNT, the CPP performed additional experiments using BEGM medium (for BEAS-2B), showing that the combination of bovine serum albumin (BSA) and 1,2-dipalmitoyl-sn-glycero-3 phosphocholine (DPPC) provided optimal suspension stability (Supplemental Material, Figure S1A). In addition, since ZnO has been shown to dissolve in aqueous solutions, the CPP determined the dissolution rate of ZnO in water, BEGM, and DMEM media. At 24 h, the percentage of dissolution was 12%, 32%, and 35%, respectively (Supplemental Material, Figure S1B). Detailed protocols and extra supplementary raw data can be found at http://cehsweb.health.umt.edu/nanogo-supp-info (CEHS 2012).

Cytotoxicity of ENM

In vitro studies with ENM involved eight laboratories and included 2 phases. It should be noted that in some cases not all eight laboratories were able to report full results. For instance, some optical density readings were above 2.0, and some labs had 100% cell lysis values lower than the particle-exposed values. These data were not usable and were not included in the final results. The CPP carried out Phase I studies with previously established protocols used in the respective laboratories of the consortium members. In contrast, the CPP conducted Phase II studies using protocols developed after identifying and solving technical problems in Phase I. The CPP selected MTS and LDH assays because they are the most commonly used single endpoint cell viability assays for nanotoxicity studies in the literature (Smith et al. 2011; Wang et al. 2010; Xia et al. 2008a). The relative simplicity of the assay procedures allowed the studies to be conducted concurrently, using the supernatant from the MTS assay (which would typically be discarded if only the MTS assay was performed) to perform LDH measurements.

MTS assays

The CPP discovered substantial variations among the replicates within individual laboratories in the Phase I MTS assays using BEAS-2B and RLE-6TN cells. This is demonstrated in Figure 2A, which showed low consistency of ZnO MTS data using RLE-6TN cells in Phase I experiments. The CPP determined that ENM interfered directly with the optical density readings (left graph in Figure 2B). Therefore, the CPP eliminated the optical interference by adding a centrifugation procedure to isolate the suspended ENM at the bottom of the cell culture dish, then transferring the supernatants to a fresh plate in order to conduct the absorbance readings (right graph in Figure 2B). Figure 2C shows the Phase II results of MTS assay in RLE-6TN cells using the updated protocols, and the results showed high consistency with low variability among different laboratories.

Figures 2D and E show the combined data for the MTS assays using THP-1 cells. When comparing the ENM within each group, the CPP determined that ZnO was the most toxic followed by TiO_2-NB. None of the other ENM caused any significant toxicity as detected by the MTS assay. The combined MTS data for the BEAS-2B and RLE-6TN cells from all laboratories also showed clear toxicity trends for ZnO as shown in Supplemental Material, Figures S2A, S2C, S3A and S3C.

Figure 2F compares reproducibility of MTS assays between Phases II and I. Stratifying by ENM and cell line, the CPP found that both error in mean and measurement error were either reduced or left unchanged when comparing Phase II to Phase I data. Overall, estimations show a 30% (95% CI: 5, 51%) reduction in the error in mean between Phase I and Phase II, with significant improvement in reproducibility among laboratories. In addition, a 40% (95% CI: 13, 60%)

reduction in measurement error occurred between Phase I and Phase II, showing substantially improved within-laboratory repeatability.

LDH assays

Similar to the MTS assays, the LDH assay results in response to ZnO treatment of RLE-6TN cells improved in the second phase of testing. Three laboratories showed high baseline levels in LDH in Phase I as compared to other laboratories and did not have the same dose response patterns exhibited by the majority of the laboratories (Figure 3A). In contrast, the procedural improvements in Phase II show a much better agreement between laboratories (Figure 3B). The combined data for the LDH assays using THP-1 cells showed the same patterns of toxicity compared to the MTS assays (Figures 3C and D). The only two ENM that achieved significant toxicity using the LDH assay were TiO_2-NB and ZnO. Detailed summary LDH data for BEAS-2B and RLE-6TN cells can be found in Supplemental Material, Figures S2B, S2D, S3B and S3D.

Figure 3E reports the results comparing reproducibility of LDH assays between Phases II and I. Stratifying by ENM and cell line, the CPP found that both error in mean and measurement error were either reduced or left unchanged when comparing Phase II to Phase I data. Only one ENM by cell line combination (ZnO – RLE6TN) exhibited decreased reproducibility on average, but the difference in errors was not statistically significant. Comparatively, for the same particle by cell line combination, estimations of measurement error showed a substantial reduction (40% decrease). Overall, assessments of the improvement in assay performance showed a 13% (95% CI: -0.12, 42%) improvement in reproducibility and 21% (95% CI: -0.09, 53%) improvement in repeatability.

Inflammatory Potential of ENM

The above studies demonstrated that only ZnO (all models tested) and TiO_2-NB (THP-1 only) caused *in vitro* cytotoxicity. Since cytotoxicity does not necessarily translate mechanistically to *in vivo* pathology, the consortium studies included measurement of NLRP3 inflammasome generated IL-1β from THP-1 cells. The results of the Phase I experiments measuring IL-1β production using THP-1 cells demonstrated that only two laboratories showed a significant increase from TiO_2-NB treatment (Figure 4A). The CPP determined that the inter-laboratory inconsistency in the Phase I experimental results was possibly due to cell clumping and excessive cell death when using PMA alone for differentiation (left graph in Figure 4B). In order to improve data consistency, the CPP modified the macrophage differentiation method by using Vitamin D_3 followed by a lower concentration of PMA (Figure 4B the right graph). Figure 4C shows that after using the improved protocols in Phase II studies, all laboratories reported significant increases in IL-1β production in THP-1 cells in response to TiO_2-NB.

Figures 4D and 4E show the combined data from the Phase I and Phase II studies, respectively. The large error bars in Phase I were due to the sizeable between-lab variation shown in Figure 4A. Consequently, only TiO_2-NB caused a nonsignificant dose-dependent IL-1β release. In contrast, in Phase II the combined data demonstrated that TiO_2-NB caused a significant IL-1β release from THP-1 cells and MWCNT also increased IL-1β release although the results did not achieve significance when all laboratories were averaged. The between-lab variance and the large effect of the TiO_2-NB negated any significance of the MWCNT IL-1β dose-dependent increases shown in Figure 4E. However, consideration of the individual laboratory data showed a significant dose-dependent increase for the O-MWCNT in all but 2 labs (Supplemental Material, Figure S4). In every case, ranking the bioactivity of the MWCNT

resulted in the following order: O-MWCNT > P-MWCNT > F-MWCNT. The probability of this rank order occurring in every lab by chance was $P < 0.001$. In contrast ZnO, which was the most cytotoxic of the ENM, did not cause any apparent IL-1β release regardless of dose (Figure 4E).

Figure 4F shows the results comparing reproducibility of IL-1β assays between Phases II and I. Stratifying by ENM, comparisons of Phase II and Phase I data show a reduction in both error in mean and measurement error. Combination of all ENM and cell lines showed an estimated 74% (95% CI: 41, 95%) reduction in the error in mean and significant improvement in reproducibility among laboratories. Furthermore, within-laboratory repeatability improved substantially with an 83% (95% CI: 63, 99%) reduction in measurement error.

Discussion

The NIEHS consortium conducted this study in an effort to identify and minimize sources of variability among laboratories performing *in vitro* testing of ENM. Eight laboratories participated in all or part of two rounds (Phase I and Phase II) of *in vitro* tests using cell lines and ENM types that were collectively selected by consortium members. After identification of several technical problems in Phase I, the CPP significantly improved the inter-laboratory variability in Phase II. Furthermore, conclusions on the relative potency of the different ENM for both toxicity and bioactivity will contribute to the information necessary to help predict relative risk for the ENM. In addition, results showed the MTS assay to be comparable in data quality and predictive value when compared to the LDH assay for toxicity testing.

A significant finding of this study was that the development of harmonized *in vitro* assay protocols made it possible to achieve reproducible results among different laboratories. This

study was among the first attempts of large scale round robin tests of ENM at the national and international level. There have been reports of a successful effort to perform inter-laboratory comparisons to characterize ENM by establishing detailed shipping, measurement, and reporting protocols (Lamberty et al. 2011; Roebben et al. 2011). Specifically, researchers demonstrated a reduction in inter-laboratory variations, especially for dynamic scattering measurements (Roebben et al. 2011). In comparison, the current study outlined a novel method of *in vitro* testing using multiple cell types, ENM and assays.

The planning of these *in vitro* tests included steps to control for many factors. For example, protocol development included consideration of varying cell culture conditions, cell type, number and cell viability, assay protocols, and most importantly, experience of the scientist that actually performed the experiments. To this end, the CPP obtained cells and reagents from the same batch or lot number and followed a detailed cell culture and assay protocol for each experiment. Investigators and laboratory personnel established a mechanism to communicate with others and to share their experience in performing specific assays. The frequent communication was very helpful for achieving reproducible results within and among the laboratories.

The strategies established for inter-laboratory communication provided a foundation for the development of more effective protocols during Phase II studies in order to account for the inherent difficulties in evaluating ENM. For example, through close communication, the CPP determined that ENM interfere with optical density readings--creating artifacts and erroneous high MTS values (Kroll et al. 2012). The Phase I MTS assay protocol, as based on the Promega manufacturer's instructions, did not take into consideration potential absorbance anomalies created by the ENM. As a result, although the combined Phase I MTS assays showed clear

toxicity profiles of TiO_2-P25, TiO_2-A, TiO_2-NB, and ZnO in RLE-6TN and BEAS-2B cells (Supplemental Material, Figures S2, S3), a large variation existed among the laboratories, as shown in Figure 2A. The CPP determined this anomaly to be due to the presence of residual ENM following treatment of the cells, as demonstrated in Figure 2B. Therefore, the Phase II protocol introduced a simple centrifugation step and media removal after MTS reagent incubation, thus allowing the absorbance to be read using supernatant containing ENM-free MTS solution. This additional step eliminated the ENM interference with the assay and significantly improved the intra- and inter-laboratory consistency.

The CPP determined ENM interference to be only one potential source of variability for *in vitro* assays. Phase I results of the LDH and IL-1β assays clearly demonstrated that cell culture conditions also contributed to the observed variability. Stimulated release of IL-1β from THP-1 cells relied in part on the activation and differentiation of THP-1 cells by high levels of PMA in the Phase I protocol. PMA induced strong responses in THP-1 cells resulting in severe clumping of the THP-1 cells during the activation process, in addition to excessive cell death occurring upon scraping the cells. Using this protocol, only two laboratories demonstrated toxicity of TiO_2 nanobelts in the MTS and LDH assays or inflammasome activation in the IL-1β assay in the Phase I tests. However, by replacing some of the PMA with Vitamin D_3, a milder signal for THP-1 activation, the cells remained well dispersed. Consequently, Phase II results demonstrated similar results for IL-1β production by THP-1 cells stimulated with TiO_2-NB between laboratories.

Consortium efforts found that the MTS assay was at least equal in reliability to assess ENM toxicity as the LDH assay. Both toxicity assays tracked each other very well for the different

ENM and cell types. Although this finding needs further validation, it suggests that the easy-to-conduct MTS assay could serve as a highly reliable testing method for *in vitro* studies of ENM-induced cytotoxicity when conducted as described in the Phase II protocol (supplemental information http://cehsweb.health.umt.edu/nanogo-supp-info (CEHS 2012)). The observation that there was a difference in the relative potency between TiO_2-NB and ZnO between the two assays is likely not as important as the observation that both were significantly cytotoxic *in vitro* suggesting that both ENM should be tested *in vivo*.

The consortium studies also provided reproducible findings of relative toxicity and bioactivity of the various ENM across the different cell lines. For example, ZnO was highly toxic to all three cell types examined in this study, yet did not stimulate inflammasome activity in THP-1 cells (Figure 4), suggesting that cytotoxicity and bioactivity (e.g., stimulation of inflammasome-mediated IL-1β release) do not necessarily correlate. Studies on inflammation and lung pathology implicate the importance of inflammasome generated IL-1β production (Cassel et al. 2008; Dostert et al. 2008; Franchi et al. 2009; Tschopp and Schroder 2010). In addition, a consortium laboratory recently demonstrated the importance of IL-1β release in generating an inflammatory response to MWCNT *in vivo* (Girtsman et al. 2012). Therefore, the CPP recommend the inclusion of mechanism-linked bioactivity assays along with traditional cytotoxicity assays for *in vitro* ENM screening.

The two forms of TiO_2 nanospheres (P25 or A) were not significantly cytotoxic or bioactive, yet TiO_2-NB were highly cytotoxic and selectively induced inflammasome activity towards THP-1 cells, consistent with previous studies (Hamilton et al. 2009). The lack of toxicity of the TiO_2-NB towards epithelial cells can probably be explained by their poor internalization of the

material, and suggests that if *in vitro* studies were conducted solely with epithelial cell lines such as those used in this study, the high toxicity of this material would not have been identified. Consequently, an important recommendation is to conduct studies with multiple relevant cell types to avoid false negative outcomes.

In parallel with the *in vitro* studies, another consortium effort amongst seven different laboratories conducted *in vivo* studies utilizing rats, mice and most of the ENM described in the present study. These researchers performed similar efforts to address technical issues and methods to reduce variability (Bonner et al. 2013). The CPP *in vitro* TiO_2 studies predicted the *in vivo* outcomes with more laboratories observing significant lung inflammation with the TiO_2-NB compared to the two nanosphere forms. The results presented in this study are also consistent with a recent report demonstrating that TiO_2-NB, but not nanospheres caused lung fibrosis (Porter et al. 2013). Furthermore, observations showed a greater activity of O-MWCNT compared to P-MWCNT or F-MWCNT. Therefore, the *in vitro* studies had the potential to accurately predict the relative potency for the TiO_2 materials observed *in vivo*. In fact, the IL-1β (proxy measure for NLRP3 inflammasome) result from this study would predict that the TiO2-NB and the O-MWCNT would be the two ENM that would result in lung pathology, and that was confirmed in the corresponding *in vivo* work (Bonner et al. 2013).

Conclusions

These studies strived to improve concordance of test results among laboratories while ensuring that the assays are predictive of *in vivo* outcome. The CPP achieved the goal to produce reliable and repeatable *in vitro* toxicity testing for ENM, however improvement in the predictability of the assays is still a work in progress. Care needs to be taken to understand the limitation of *in*

vitro testing and not to over-interpret *in vitro* studies without comprehensive companion *in vivo* studies. These studies utilized well-characterized nanomaterials, including a positive and negative control, in addition to a well-established dispersion protocol ensuring stable suspensions in cell culture media. This consortium effort provided a series of harmonized protocols and tested models for the nanotoxicological field to use. The results also demonstrated that toxicity and inflammasome activity did not always track each other and that different cell types yielded different estimates of safety of different ENM. Consequently, future studies should utilize multiple endpoints and multiple cell types to avoid false negative results. Finally, this effort serves as a good template for future endeavors in the field of nanotoxicology, providing key elements necessary for collaborative efforts between laboratories.

References

Bonner JC, Silva RM, Taylor AJ, Brown JM, Hilderbrand SC, Castranova V, et al. 2013. Interlaboratory evaluation of rodent pulmonary responses to engineered nanomaterials. Environ Health Perspect (In press).

Cassel SL, Eisenbarth SC, Iyer SS, Sadler JJ, Colegio OR, Tephly LA, et al. 2008. The nalp3 inflammasome is essential for the development of silicosis. Proc Natl Acad Sci U S A 105:9035-9040.

CEHS. 2012. Nanogo supplemental information. Available: http://cehsweb.health.umt.edu/nanogo-supp-info [accessed February 10, 2013].

Chen YH, Mitra S. 2008. Fast microwave-assisted purification, functionalization and dispersion of multi-walled carbon nanotubes. J Nanosci Nanotechno 8:5770-5775.

Dostert C, Petrilli V, Van Bruggen R, Steele C, Mossman BT, Tschopp J. 2008. Innate immune activation through nalp3 inflammasome sensing of asbestos and silica. Science 320:674-677.

Driscoll KE, Carter JM, Iype PT, Kumari HL, Crosby LL, Aardema MJ, et al. 1995. Establishment of immortalized alveolar type ii epithelial cell lines from adult rats. *In vitro* Cell Dev Biol Anim 31:516-527.

Franchi L, Eigenbrod T, Munoz-Planillo R, Nunez G. 2009. The inflammasome: A caspase-1-activation platform that regulates immune responses and disease pathogenesis. Nat Immunol 10:241-247.

Girtsman TA, Beamer CA, Wu N, Buford M, Holian A. 2012. Il-1r signalling is critical for regulation of multi-walled carbon nanotubes-induced acute lung inflammation in c57bl/6 mice. Nanotoxicology.

Hamilton RF, Wu N, Porter D, Buford M, Wolfarth M, Holian A. 2009. Particle length-dependent titanium dioxide nanomaterials toxicity and bioactivity. Part Fibre Toxicol 6:35.

Ji Z, Jin X, George S, Xia T, Meng H, Wang X, et al. 2010. Dispersion and stability optimization of tio2 nanoparticles in cell culture media. Environ Sci Technol 44:7309-7314.

Kroll A, Pillukat MH, Hahn D, Schnekenburger J. 2012. Interference of engineered nanoparticles with *in vitro* toxicity assays. Archives of Toxicology 86:1123-1136.

Lamberty A, Franks K, Braun A, Kestens V, Roebben G, Linsinger TPJ. 2011. Interlaboratory comparison for the measurement of particle size and zeta potential of silica nanoparticles in an aqueous suspension discussion. J Nanopart Res 13:7317-7329.

Maynard AD, Aitken RJ, Butz T, Colvin V, Donaldson K, Oberdorster G, et al. 2006. Safe handling of nanotechnology. Nature 444:267-269.

Meng H, Xia T, George S, Nel AE. 2009. A predictive toxicological paradigm for the safety assessment of nanomaterials. ACS Nano 3:1620-1627.

Nel A, Xia T, Madler L, Li N. 2006. Toxic potential of materials at the nanolevel. Science 311:622-627.

Oberdorster G, Oberdorster E, Oberdorster J. 2005. Nanotoxicology: An emerging discipline evolving from studies of ultrafine particles. Environmental health perspectives 113:823-839.

Porter D, Sriram K, Wolfarth M, Jefferson A, Schwegler-Berry D, Andrew M, et al. 2008. A biocompatible medium for nanoparticle dispersion. Nanotoxicology 2:144-154.

Porter DW, Wu N, Hubbs AF, Mercer RR, Funk K, Meng F, et al. 2013. Differential mouse pulmonary dose and time course responses to titanium dioxide nanospheres and nanobelts. Toxicol Sci 131:179-193.

Roebben G, Ramirez-Garcia S, Hackley VA, Roesslein M, Klaessig F, Kestens V, et al. 2011. Interlaboratory comparison of size and surface charge measurements on nanoparticles prior to biological impact assessment. J Nanopart Res 13:2675-2687.

Sager TM, Porter DW, Robinson VA, Lindsley WG, Schwegler-Berry DE, Castranova V. 2007. Improved method to disperse nanoparticles for *in vitro* and *in vivo* investigation of toxicity. Nanotoxicology 1:118-129.

Smith SM, Wunder MB, Norris DA, Shellman YG. 2011. A simple protocol for using a ldh-based cytotoxicity assay to assess the effects of death and growth inhibition at the same time. PLoS One 6:e26908.

Tschopp J, Schroder K. 2010. Nlrp3 inflammasome activation: The convergence of multiple signalling pathways on ros production? Nat Rev Immunol 10:210-215.

Wang X, Xia TA, Ntim SA, Ji ZX, George S, Meng HA, et al. 2010. Quantitative techniques for assessing and controlling the dispersion and biological effects of multiwalled carbon nanotubes in mammalian tissue culture cells. ACS Nano 4:7241-7252.

Wang X, Xia T, Ntim SA, Ji Z, Lin S, Meng H, et al. 2011. Dispersal state of multiwalled carbon nanotubes elicits profibrogenic cellular responses that correlate with fibrogenesis biomarkers and fibrosis in the murine lung. ACS Nano 5:9772-9787.

Xia T, Kovochich M, Liong M, Madler L, Gilbert B, Shi HB, et al. 2008a. Comparison of the mechanism of toxicity of zinc oxide and cerium oxide nanoparticles based on dissolution and oxidative stress properties. ACS Nano 2:2121-2134.

Xia T, Kovochich M, Liong M, Zink JI, Nel AE. 2008b. Cationic polystyrene nanosphere toxicity depends on cell-specific endocytic and mitochondrial injury pathways. ACS Nano 2:85-96.

Table 1: Physicochemical characterization of TiO_2 and ZnO ENM (± indicates mean ± s.d.).

Quality	**Technique**	**P25**	**Anatase**	**Nanobelts**	**ZnO**
Size (nm)	TEM	~24	~28	L:7000; W:200; T:10	~20
Size in H_2O (nm) (intensity-based)	DLS	209±8 (PdI 0.065)	292±70	2897±117	215±15 (PdI 0.033)
Phase & Structure	XRD	81% anatase and 19% rutile	100% anatase	100% anatase	100% Zincite
Shape/Morphology	TEM	Spheroid	Spherical	Belt	Spheroid
Surface Area (m^2/g)	BET	53	173	18	26
Zeta Potential in H2O at pH 6.0 (mV)	Zetasizer	-34.4±1.6	-30.7±0.8	-30.3±2.8	-28.2±0.5
Elemental Analysis (wt.%)	ICP-MS	98.6	n/a	n/a	99.3

L: length; W: width; T: thickness; n/a: not available.

Table 2: Physicochemical characterization of MWCNT (± indicates mean ± s.d.)

Quality	**Technique**	**O-MWCNT**	**P-MWCNT**	**F-MWCNT**
Size (nm)	TEM	D: 20–30; L: 5000–10000	D: 20–30; L: 5000–10000	D: 20–30; L: 5000–10000
Size in H_2O (nm) (intensity-based)	DLS	324±33	858±58	234±24
Shape/Morphology	TEM	Nanotube	Nanotube	Nanotube
Surface Area (m^2/g)	BET	180	513	26
Zeta Potential in H2O at pH 6.0 (mV)	Zetasizer	-12.1±0.3	-11.8±1.1	-48.4±1.7
Elemental Analysis (wt.%)	ICP-MS	4.5% Ni, 0.8% Fe	1.8% Ni, 0.1% Fe	0.2% S

L: Length, D: Diameter

Figure Legends

Fig 1: SEM images of all selected ENM. From top left: TiO_2-P25, TiO_2-NB, TiO_2-A, and ZnO. From bottom left: O-MWCNT, P-MWCNT, and F-MWCNT. Scale indicated by the bars.

Fig 2: Phase I/II comparisons for RLE-6TN and THP-1 cells using MTS assay data. A) Percent viable RLE-6TN cells relative to no particle control for each individual lab in Phase I. B) Illustration of how the ENM distorts optical density readings in the MTS assay. Left panel: OD readings with the ENM in the culture well. Right panel: OD readings with the media supernatant removed and replaced in wells without particle interference. C) Percent viable RLE-6TN cells relative to no particle control for each individual lab in Phase II. D) Percent viable cells relative to no particle control for THP-1 Phase I conditions. E) Percent viable cells relative to no particle control for THP-1 Phase II conditions. F) Line graphs illustrating the changes in *error of the mean* and *measure in error* from Phase I to Phase II trials for MTS assay data. Data expressed as means ± SEM; * indicates significance at $P < 0.05$ compared to other particles at the same concentration and/or the "no particle" control.

Fig 3: Phase I/II comparisons for RLE-6TN and THP-1 cells using LDH assay data. A) Percent LDH release in RLE-6TN cells relative to total cell lysis (100% cell death) for each individual lab in Phase I. B) Percent LDH release in RLE-6TN cells relative to total cell lysis (100% cell death) for each individual lab in Phase II. C) Percent LDH release relative to total lysis (100% cell death) for THP-1 Phase I conditions. D) Percent LDH release relative to total lysis (100% cell death) for THP-1 Phase II conditions. E) Line graphs illustrating the changes in *error of the mean* and *measure in error* from Phase I to Phase II trials for LDH assay data. Data

expressed as means ± SEM; * indicates significance at $P < 0.05$ compared to other particles at the same concentration and/or the "no particle" control.

Fig 4: Phase I/II comparisons for THP-1 cells using IL-1β assay data. A) Percent IL-1β release from THP-1 cells for each individual lab in Phase I. B) Illustration of how the THP-1 cell differentiation technique altered cell morphology. Left panel: THP-1 cells pretreated with PMA for 24 hr created clumped cells. Right panel: THP-1 cells pretreated with Vitamin D3 for 24 hr created evenly dispersed cells. C) IL-1β release from THP-1 cells for each individual lab in Phase II. D) Summary IL-1β release for Phase I conditions. E) Summary IL-1β release for Phase II conditions. F) Line graphs illustrating the changes in *error of the mean* and *measure in error* from Phase I to Phase II trials for IL-1β assay data. Data expressed as means ± SEM; * indicates significance at $P < 0.05$ compared to other particles at the same concentration and/or the "no particle" control. Asterisks *** indicate significance at $P < 0.001$ for significant dose-response (each labs data analyzed independently).

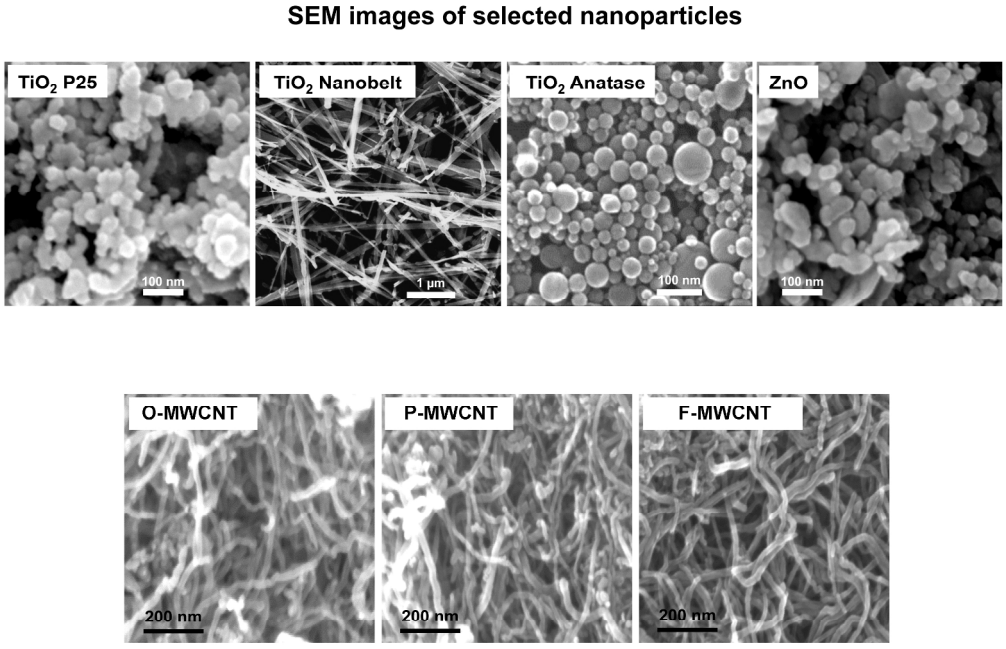

Figure 2
254x190mm (300 x 300 DPI)

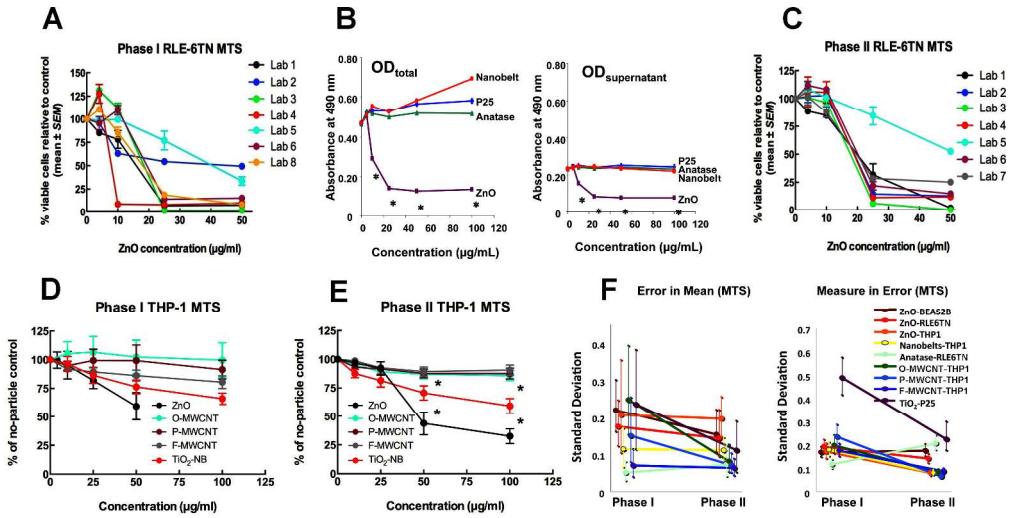

Figure 2
355x180mm (300 x 300 DPI)

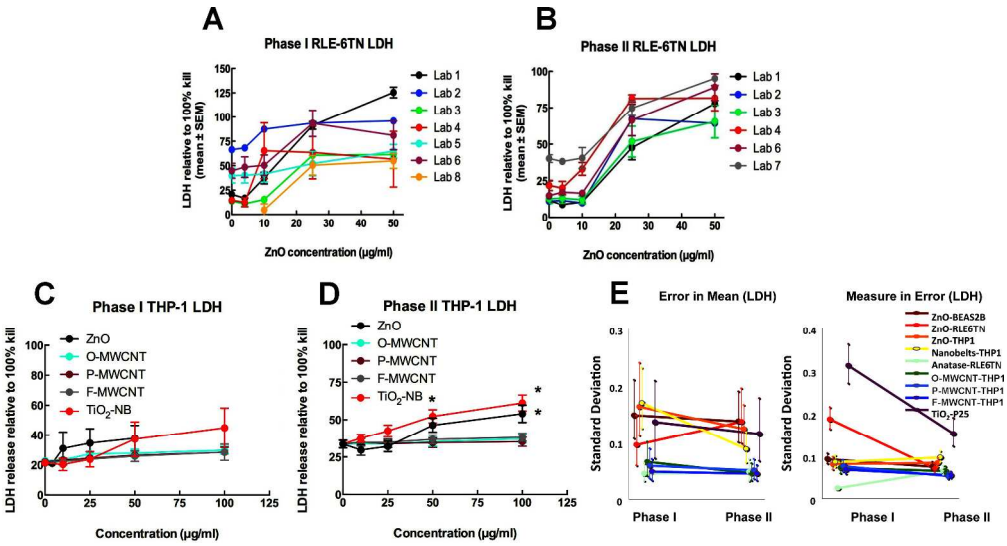

Figure 3
340x182mm (300 x 300 DPI)

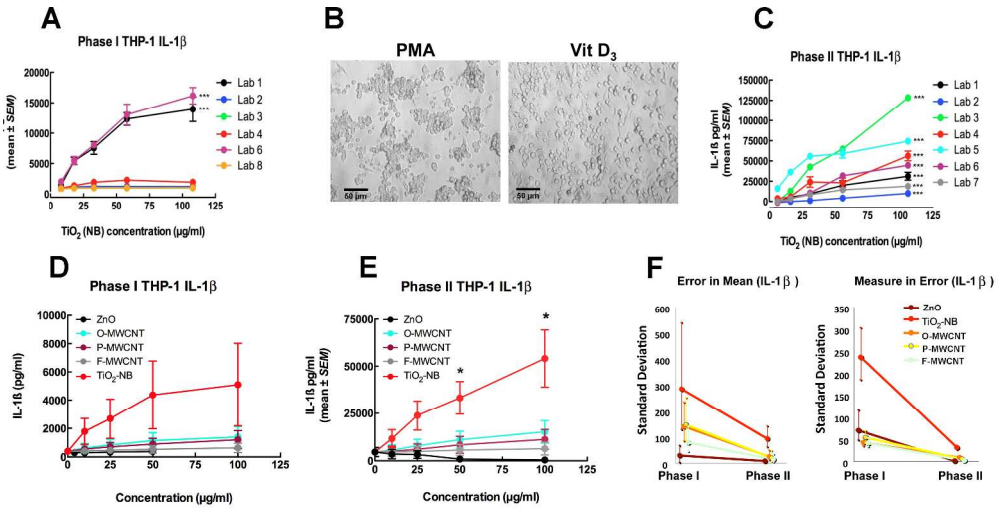

Figure 4
359x180mm (300 x 300 DPI)